

Experimental report

02/09/2021

Proposal: 9-12-625

Council: 4/2020

Title: Lipid Interaction with Styrene Maleic Acid Copolymers on Gold Nanoparticles

Research area: Chemistry

This proposal is a new proposal

Main proposer: Karen EDLER

Experimental team: Sylvain PREVOST

Local contacts: Sylvain PREVOST

Samples: Au nanoparticles
styrene-maleic acid copolymer on Au nanoparticles
DMPC in phosphate buffer
d54-DMPC in phosphate buffer

Instrument	Requested days	Allocated days	From	To
D11	2	2	21/03/2021	23/03/2021
D22	2	0		
D33	2	0		

Abstract:

Polymer stabilized lipid nanodiscs can be used to extract and stabilize membrane proteins in solution for structural studies. Previously, we studied nanodisc formation using poly(styrene-maleic acid) (SMA) copolymers synthesised by RAFT techniques, which give defined weights and architectures, and also have thiol end groups that may be used for surface binding. We have now shown that SMA tethered to gold nanoparticles will solubilise lipid vesicles. By tethering SMA to relevant nanoparticle surfaces, such as conductive gold nanoparticles the applications of SMA-nanodiscs could be broadened towards sensors for protein binding or developed for use as a membrane protein separation system. However, it seems unlikely that a polymer tethered to a nanoparticle will form disc-like structures in the same way as this system does in solution. Here, we aim to use SANS and contrast variation to determine the surface structures that develop when tethered SMA polymers bind lipids in this system, and how these compare with known SMALP nanodisc morphologies. We will also vary the position of the styrene block relative to the surface to identify how this alters bound lipid structures.

1.0 Objectives & Experimental

Styrene (Sty) maleic acid (MA) copolymers (SMA) prepared via RAFT polymerisation have been found to disrupt cell membranes and form lipid nanodiscs by self assembly (SMALPs). By tethering the active copolymer to functional metallic interfaces, such as gold nanoparticles (AuNPs), it is hoped that the applications of SMA may be expanded. Initial work has indicated that the behaviour of SMA at these interfaces can be influenced by the copolymer block architecture synthesised perpendicular from the surface. Here, we aimed to investigate the structures formed by these systems upon interaction with variant lipid species, including examination of the effects of block architecture, surface identity and lipid phase.

A one-pot synthesis of SMA (2:1 monomer ratio) by the controlled polymerisation technique, RAFT, typically yields copolymers composed of a strictly alternating Sty-MA block, followed by a Sty homoblock. Three block architectures of SMA were synthesised for this experiment, including both hydrogenated (h) and partially deuterated (d) variants using d_8 -Styrene. This included *forward* SMA (h/dSMA), where the polymer is tethered by the Sty homoblock with the alternating block extended in solution, *reverse* SMA (hr/drSMA), with the Sty homoblock instead in solution, and *triblock* (ht/dtSMA), with a Sty homoblock both tethered and in solution. Two NP species were used, AuNPs and super paramagnetic iron oxide nanoparticles (SPIONs) to explore the effects of varied physiochemical properties at the interface. Likewise, three lipid species were used, hDMPC, dDMPC ($T_m \sim 24^\circ\text{C}$), and hDPPC ($T_m \sim 41^\circ\text{C}$). The experimental temperature was set at 26°C , and hence this allowed examination of how the phase and identity of the lipid affected self assembly. For any system where a polymer was deuterated, this was interacted with a hydrogenated lipid species, and *vice versa*, to provide contrast.

All systems were measured at at least three contrasts (100%, 85%, 76%, 50% or 35% D_2O) where effective contrasts for the various systems had been identified previously from SANS experiments (ISIS, UK). Preparatory investigation found that the relevant size range for these systems was broad (10-20 nm for the metallic particles; 80-100 nm for the polymer-lipid shell). Hence, three detector distances were used to measure the desired q-range ($0.0007 - 0.5\text{\AA}^{-1}$). Data work up and analysis is currently ongoing and contrasts will be fit simultaneously using the *NIST SANS Analysis* package within *Igor Pro*.

2.0 Report

2.1 Gold Nanoparticles (Au-NPs)

As the proposed systems were composed of a mixture of interacting species, it was desirable to initially characterise their constituent components as to distinguish the emergence of new structures. Figure 1A presents the data for the polymer-only aggregates in solution at 1 mg ml^{-1} , representing the expected polymer loading of the nanoparticles. Hence, scattering arising from any polymer not tethered to metallic nanoparticles in subsequent experiments may be discerned. Here, it appears that the reverse and triblock configurations cause polymer aggregation, as indicated by the steeper gradient at low-q. Likewise, Figure 1B presents the scattering from hDPPC SUVs, and Figure 2B the scattering from dDMPC SUVs. At 26°C , whereas the hDPPC SUVs were aggregating slightly, the dDMPC SUVs were not.

Previous experiments characterised the interaction between Au-hSMA and Au-rSMA with DMPC vesicles, and here, these particles were interacted with hDPPC SUVs to discern any difference to behaviour. In neither case could a signal be detected for just the Au-polymer particles, as can be seen for Au-htSMA (Figure 1E), given the large absorbance cross-section of gold. However, previously when Au-h/rSMA was interacted with DMPC vesicles, discernable features arose. Here, activity with DPPC can also be implied from the features that arise upon interaction (Figure 2C-D), distinct from those found in the data for DPPC SUVs alone (Figure 1B), suggesting a structural change. The gold nanoparticle and polymer shell are represented by the small bump at around $q = 0.1\text{\AA}^{-1}$ in D_2O , now visible due to contrast against the lipids. Likewise, the radius of the larger lipidic structure or vesicle is given by the broad bump that drops off between $0.003\text{-}0.01\text{\AA}^{-1}$. In the hDPPC SUV sample, this occurred at $q = 0.007\text{\AA}^{-1}$ and was shifted to $q = 0.004\text{\AA}^{-1}$ and $q = 0.01\text{\AA}^{-1}$ for Au-dSMA and Au-drSMA, respectively. Hence, not only does Au-SMA interact with DPPC, this occurred differently to the interactions with DMPC, and again appears to be influenced by copolymer block

architecture.

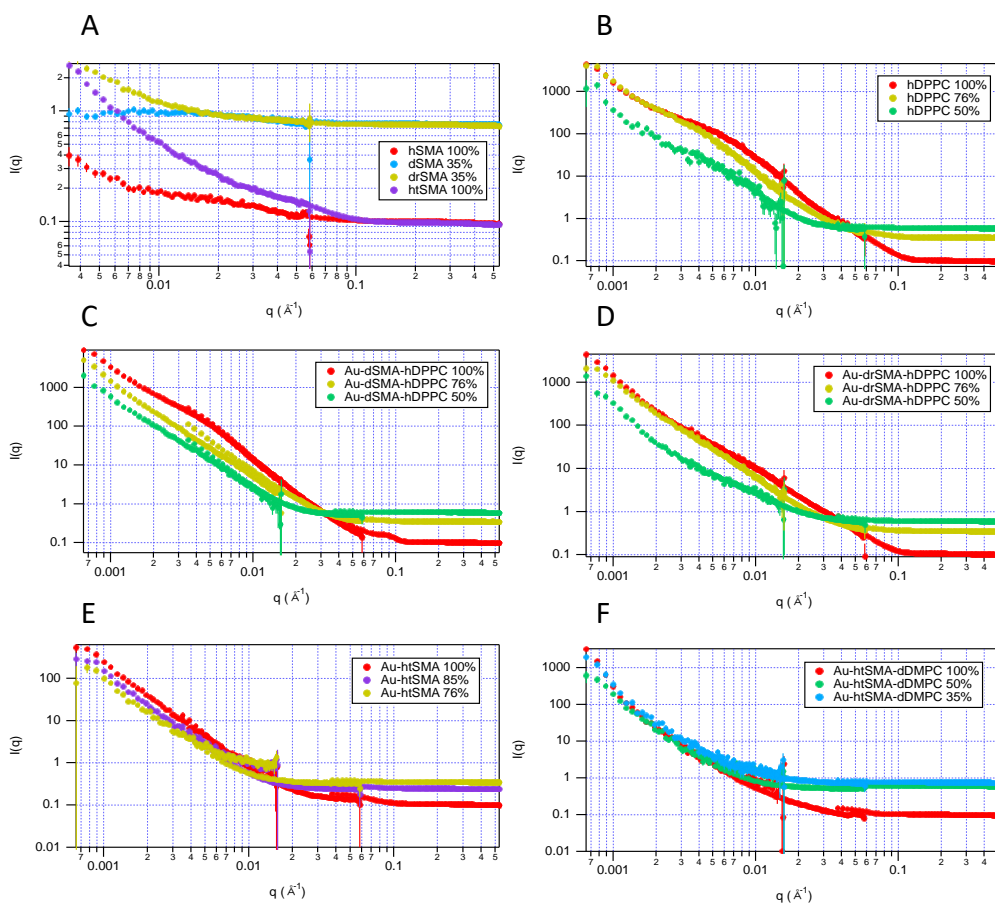


Figure 1: SANS data for (A) SMA aggregates (1 mg ml^{-1}). (B) hDPPC small unilamellar vesicles (SUVs) (1 mg ml^{-1}). (C-D) Au-SMA after interaction with DPPC. (E) Au-htSMA before and (F) after incubation with dDMPC SUVs.

As mentioned previously, scattering from Au-htSMA alone was very weak, making it difficult to discern any structure. However, interestingly, no features arose upon interaction with dDMPC either. This was unexpected, as other results (DLS, SAXS etc.) previously indicated an interaction. It may be that the particles were too large to be reasonably addressed by the q -range here. A slight down turn can be seen at low- q (Figure 1E) indicating a relatively large structure. Another possibility is that the triblock system was unstable. There is mismatch between the q -ranges of the different detector distances, suggesting structural changes over the timeframe of measurement. Similarly, aggregation was indicated at low- q , as for all systems presented in Figure 1. Regardless, this again indicates a behavioural difference induced by only slight alterations to the copolymer architecture.

2.2 Super Paramagnetic Iron Oxide Nanoparticles (SPIONs)

The same strategy was employed to investigate the interaction between SPION-SMA systems and h/dDMPC SUVs. Bare vesicles are presented in Figures 2A-B and bare SPION-h/dSMA presented in Figures 2E-F.

As with the gold, scattering from the bare SPION-SMA particles was quite weak, although discernable. This can be seen from the broad bump in D_2O in both systems, at approximately $q = 0.003 \text{ \AA}^{-1}$, indicative of a structure much larger than the typical 10 nm diameter of the SPIONs measured previously (DLS, SAXS, TEM). Hence, the suspension was likely in an aggregating state given the superparamagnetism of the particles, as indicated by the steep gradient at low- q and mismatch between detector distances. However, these systems appeared to stabilise upon the addition of DMPC SUVs (Figures 2C-D). This produced new features, most dramatically in the SPION-dSMA-hDMPC system. It is believed that the oscillations in the q -range $0.006\text{-}0.03 \text{ \AA}^{-1}$ relate to a well-defined core-shell sphere structure. It can be seen that both systems are now aggregating versus the bare SUVs which were not. Furthermore, size changes to the vesicles were again indicated from

the shift of the peaks, and a possible shape change (aspect ratio; sphere to ellipse) from the change in q -dependency at mid- q . Hence, tentatively, the data indicates a positive interaction of DMPC SUVs with SPIONs-SMA, producing yet different structures as were seen with the Au-SMA systems. Fitting will elucidate the structural differences apparent within these systems, allowing for their rational optimisation and implementation.

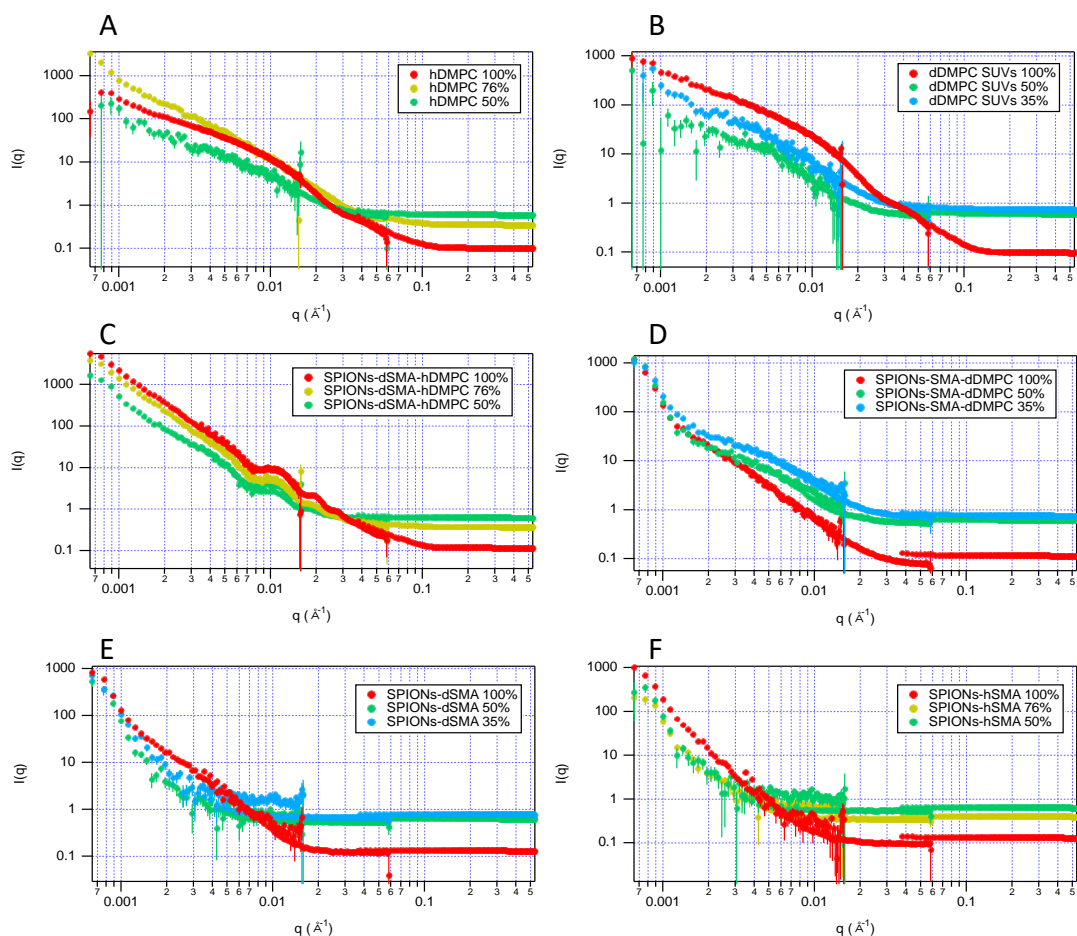


Figure 2: SANS data for (A-B) DMPC SUVs (1 mg ml^{-1}). (C-D) SPIONs-SMA after interaction with DMPC SUVs. (E-F) SPIONs-SMA before interaction with DMPC SUVs.

3.0 Conclusions

In both the Au-SMA and SPION-SMA systems strong interactions with DMPC and DPPC are seen for all of the different polymers used, resulting in a variety of different structures depending on the nature of the lipid or polymer on the nanoparticle. Fitting of this data is ongoing, and will be combined with data from other techniques including SAXS, DLS, electron microscopy and QCM-D to help determine the structures and interactions in these systems. The data will form part of the PhD thesis of George Neville and we expect at least one publication to result from this work in due course.